SCHEDAE INFORMATICAE
VOLUME 20(2011) DOI 10.4467/20838476SI.11.008.0294

An Improvement in Fuzzy Entropy Edge Detection for X-ray Imaging

Tomasz Wójtowicz
Institute of Computer Science, Jagiellonian University
Łojasiewicza 6, 30-348 Krakow, Poland
e-mail: *Tomasz.Wojtowicz@ii.uj.edu.pl@ii.uj.edu.pl*

Abstract. The following paper discusses the topic of edge detection in X-ray hand images. It criticises the existing solution by highlighting a design fault, which is a carelessly chosen function and then proposes a way to eliminate the fault by replacing it with a better suited function. The search for this function and its results are also discussed in this paper. It also presents the aspect of pre- and postprocessing through filtering as another improvement in edge detection.

1. Introduction

Hand radiographs are source of important clinical information. There are number of inflammatory as well as non-inflammatory diseases within the scope of rheumatology and diagnostic radiology. Very often pathological changes are found in a palm region [1]. To make X-ray pictures examination more precise, the process of their analysis should be automated. Therefore algorithms able to handle this task are being developed, studied and implemented. Certain methods have been proposed: of X-ray pictures preprocessing [2, 3, 4], of recognition and representation of regions of interests like a bone contour or joint space [5, 6], of detection of pathological changes like joint space narrowing, bone contour change [7, 8, 9, 10, 11, 12, 13, 14]. Further advanced reasearch is based on pattern recognition and image understanding [15, 16, 17] and aims to create software for computer-aided medical diagnostics [18].

Contemporary methods of X-ray picture preprocessing, while promissing, are far from being satisfactory. This paper describes a new attempt to this task which

seems to be better that previously tested methods. The exact field of interest are X-ray images of human hands. The X-ray images are obtained in so called indirect process and result in 2320×2920 monochrome images of 16-bit depth of gray.

Processing of X-ray images is a task essentially harder than images taken in visible spectrum. Firstly, the images display a very high level of noise, resulting in the fact that an algorithm may easily mistake a noise artifact for an anatomical feature. Secondly, the images have a very low contrast understood as a difference between the foreground and background luminance, which causes simple edge detection algorithms to fail. Thirdly, due to an obvious difference in thickness, the finger area is darker than the carpal area, rendering simple binarisation algorithms useless.

To combat the first issue, this paper proposes a two stage filtering, first in prepocessing and the second in postprocessing using a median and minimum filter, respectively. This topic is discussed in Section 3.

The second and third issues are solved using a *fuzzy entropy direction feature image edge detection* multi-stage algorithm. This paper discusses only the first stage of this algorithm, i.e. the calculation of fuzzy entropy. This method was proposed in [19] and later in [20] upon which this paper relies. However, while implementing according to [20] it has shown up that the algorithm proposed therein bears a serious design fault. The theoretical aspect of this fault is discussed in Section 2 and the practical research towards its elimination is presented in Section 4.

Finally, a modified method from [20] coupled with pre- and postfiltering gives satisfactory results in the aspect of edge detection in X-ray hand images.

2. Fuzzy entropy calculation

The following formulas are directly taken from [20]. $E(p)$ is the entropy value for a given image pixel p and $N(p)$ is its neighborhood so that $p \in N(p)$. In this paper it is assumed that $N(p)$ is a 9-element square of 3×3 pixels.

$$E(p) = \frac{1}{\#N(p)} \sum_{v \in N(p)} H(U(v,p)), \tag{1}$$

where the functions are as following:

$$U(v,p) = \frac{1}{1 + |\lambda(v) - \lambda(p)|}, \tag{2}$$

$$H(x) = -x \cdot log_2 x - (1-x) \cdot log_2(1-x). \tag{3}$$

The function denoted by $\lambda()$ is a luminance value of the given pixel, which for a monochrome image is the very value of the pixel. As it was not explicitly mentioned in [20], it has been assumed that the luminance is a floating-point value in $[0, 1]$ as experiments with other ranges, e.g. $[0, 255]$, have shown not to yield usefull results. With a pixel value in $[0, 1]$ range, the function (2) returns values in the range of $[\frac{1}{2}, 1]$.

Fig. 1. An example of an original picture which is an input to the algorithm discussed herein. Observe a black overall background, grey photographic film background and a lighter hand on it. As seen especially in the fingers region, there is very small difference in luminance between the finger and the film background. Moreover, the finger area is darker than the wrist area. Both factors are among others causing the fact that X-ray image processing is an especially difficult task

The serious problem, which is the critised design fault, regards the function (3). As a fact, $log_2 0$ equals to $-\infty$, making the function (3) **incomputable** on arguments $\{0, 1\}$. It is a serious flaw, because the function (2) returns 1 when both examined pixels have identical luminance, which is a common situation.

Another problem regarding the function (3) rises from the fact that calculating a value of a logarithm is a time-consuming process. A plotted graph shows that the function (3) is a half-circle-like shape rising from point $(0, 0)$ to its maximum in $(\frac{1}{2}, 1)$ and symetrically lowering to the point $(1, 0)$. This leads to the concept of replacing function (3) with an adequatly shaped function requiring less computation effort and hopefully no incomputable points. As a replacement there were tested:

- quadratic functions (degree 2 polynomial),
- linear functions with negative slope,
- a Gauss function with $\mu = \frac{1}{2}$.

In Section 4 it was finally concluded that the quadratic function produces the best results, simultanously satisfying both allegations to the function (3), i.e. calculating

a polynomial is a time effective operation and polynomials do not have incomputable points in their domains.

3. Pre- and postprocessing

X-ray pictures have a relatively high noise. After application of an entropy calculation algorithm (1) this noise manifests itself as fake edges all over the image. In order to silence the noise a median filter is applied in preprocessing.

For a given pixel p and its neighborhood $N(p)$, such that $p \in N(p)$, a median filter is defined as following:

$$\lambda(p) = median\{\lambda(v) : v \in N(p)\}. \tag{4}$$

In the discussed solution the median filter uses a square neighborhood of 3×3 pixels. The results of preprocessing with this filter are satisfactory. After the calculation of entropy (1) the remaining noise appears as circular structures, similar to wood rings, of 1-pixel edge thickness. They can be removed in post-process filtering by a thinning operation. The thinning does not damage the important parts of the image, as all anatomical features like bones or skin are essentially thicker. To thin the picture a median filter can be used again, but a minimum filter may be a better choice.

Given pixel p and its neighborhood $N(p)$, such that $p \in N(p)$, a minimum filter is defined as following:

$$\lambda(p) = min\{\lambda(v) : v \in N(p)\}. \tag{5}$$

Again, the neighborhood for this pixel is a 3×3 square. The main argument for the minimum filter and against the median filter is running time. The minimum filter is observably faster, as it can point out the minimum value in linear time. Meanwhile, the median filter requires the set to be sorted in order to point out the middle value, and with such small sets, sorting is effectively $\Theta(n^2)$-like operation. Obviously, there are algorithms for fast median calculation, as the renowned Blum-Floyd-Pratt-Rivest-Tarjan algorithm, but such algorithms are also terribly inefficient with small sets.

On the other hand, the minimum filter produces observably darker images that the median filter. However, it was decided that a spared computation time is more important.

4. Numerical experiments

Numerical experiments regarded the pageant for the best function to replace (3). The final choice was based on the eye examination of produced output, nevertheless following numerical observables were gathered:

- E_{max} – the maximum value,
- E_{min} – the minimum value,
- $\Delta E = E_{max} - E_{min}$,
- ϕE_{pix} - the average value of E from all pixels,
- $\phi E_{val} = avg\{E_{min}, E_{max}\}$ – for comparison,
- $V = \frac{E_{pix} - E_{min}}{E_{max} - E_{min}}$ is a volume coefficient, i.e. relative amount of white.

The following table presents collected numerical data. The function (3) was slightly tuned in order to prevent the incomputability issue, as mentioned in Section 2. The sign minus following the number indicates that it has been rounded up.

Function	E_{min}	E_{max}	ΔE	ϕE_{pix}	ϕE_{val}	$V\%$
(3)	0.1985	0.3786	0.1801-	0.2028	0.2885	2.41
$x \cdot (1-x)$	0.0	0.0789-	0.0789-	0.0017-	0.0394	2.12-
$4 \cdot x \cdot (1-x)$	0.0	0.3156-	0.3156-	0.0067-	0.1578-	2.12
$40 \cdot x \cdot (1-x)$	0.0	3.1559	3.1559	0.0669	1.5780-	2.12
$400 \cdot x \cdot (1-x)$	0.0	31.5595	31.5595	0.6692-	15.7798-	2.12
$-x^2 - (1-x)^2$	-1.0	-0.8422	0.1578-	0.9966	-0.9211	2.12
$-x + 1$	0.0	0.0885	0.0885	0.0017-	0.0443-	1.91
$-2 \cdot x + 2$	0.0	0.1771-	0.1771-	0.0034-	0.0885	1.91
$10 \cdot \exp \frac{-(x-0.5)^2}{200}$	9.9875	9.9114	0.0039	9.9876-	9.9895-	2.12-

The value of entropy was then normalized, so that $[E_{min}, E_{max}]$ was proportionally mapped to the closest integer value in $[0, 255]$ in order to be dislayed on-screen. The final examination based on visual evaluation resulted with following remarks:

1. Each quadratic function gives nearly the same result. Small diferences that are the effect of rounding are neglible.
2. Linear functions give poorer results than a quadratic function.
3. Results given by Gauss and quadratic functions are very similar, hence the Gauss function is the worse choice because of its computational complexity.
4. Quadratic functions are so similar in result to (3) that they are the fine replacement.

From all the above, the $4 \cdot x \cdot (1-x)$ funciton was finally chosen as the replacement for (3).

5. Conclusion

The method proposed in this paper removes a flaw in the method discussed in the cited paper. It also improves the results of the fuzzy entropy algorithm thanks to filtering before and after the calculation of fuzzy entropy. Resulting values of entropy are themselves an image which highlights edges of a hand, therefore allowing to separate the image of a hand from the background, opening the way for other algorithms to perform further processing on it.

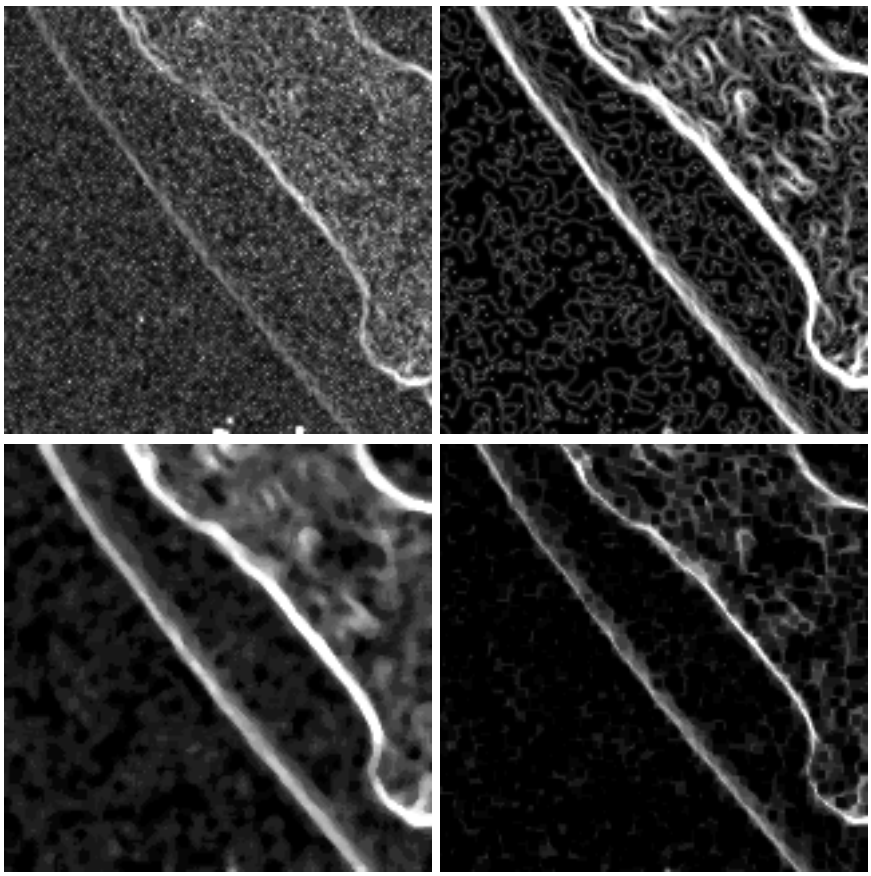

Fig. 2. Different levels of noise supression are depicted here. Upper-left – a result of pure fuzzy entropy calculation without noise supression results in a picture unusable for further processing. Upper-right – a median filter applied before fuzzy entropy calculation gives excellent contrast albeit with still visible noise. Lower-left – a median filter applied before and after calculation. Lower-right – a median before and a minimum filter applied after calculation. Whether the lower-left or lower-right picture is supposed to be the better result depends on whatever the further processing will be.

6. References

[1] Staniszewska-Varga J., Szymańska-Jagiełło W., Luft S., Korkosz M.; *Rheumatic diseases atlas (Atlas radiologiczny chorób reumatycznych)*, Medycyna Praktyczna, Kraków, 2003.

[2] Bielecki A., Korkosz M., Zieliński B.; *Hand radiographs preprocessing, image representation in the finger regions and joint space width measurements for image interpretation*, Pattern Recognition, 41(12), 2008, pp. 3786–3798.

[3] Zieliński B.; *A fully automated algorithm dedicated to computing metacarpophalangeal and interphalangeal joint cavity widths*, Schedae Informaticae, 16, 2007, pp. 47–67.

[4] Zieliński B.; *Hand radiograph analysis and joint space location improvement for image interpretation*, Schede Informaticae, 17–18, 2009, pp. 45–61.

[5] Bielecki A., Korkosz M., Wojciechowski W., Zieliński B.; *Identifying the borders of the upper and lower metacarpophalangeal joint surfaces on hand radiographs*, Lecture Notes in Computer Science, 6113, 2010, pp. 589–596.

[6] Kaufmann J., Slump C. H., Moens H. J. B.; *Segmentation of hand radiographs by using multi-level connected active appearance models*, Proceedings of the SPIE, 5747, 2005, pp. 1571–1581.

[7] Bielecka M., Bielecki A., Korkosz M., Skomorowski M. et al.; *Application of shape description metodology to hand radiographs interpretation*, Lecture Notes in Computer Science, 6374, 2010, pp. 11–18.

[8] Bielecka M., Skomorowski M., Zieliński B.; *A fuzzy shaper descriptor and interference by fuzzy relaxation with application to description of bones contours at hand radiographs*, Lecture Notes in Computer Science, 5495, 2009, pp. 469–478.

[9] Sharp J., Gardner J., Benett E.; *Computer-based methods for measuring joint space and estimating erosion volume in the finger and wrist joints of patients with rheumatoid arthritis*, Arthritis and Rheumatism, 43(6), 2000, pp. 1378–1386.

[10] Bielecka M., Bielecki A., Korkosz M., Skomorowski M. et al.; *Modified Jakubowski Shape Transducer for Detecting Osteophytes and Erosions in Finger Joints*, Lecture Notes in Computer Science, 6594, 2011, pp. 147–155.

[11] Böttcher J., Pfeil A., Rosholm A., Petrovitch A. et al.; *Digital X-ray radiogrammetry combined with semiautomated analysis of joint space widths as a new diagnostic approach in rheumatoid arthritis: a cross-sectional and longitudal study*, Arthritis and Rheumatism, 52(12), 2005, pp. 3850–3859.

[12] Pfeil A., Böttcher J., Schäfer M. L., Seidl B. E. et al.; *Normative Reference Values of Joint Space Width Estimated by Computer-aided Joint Space Analysis (CAJSA): The Distal Interphalangeal Joint*, Journal of Digital Imaging, 21(1), 2008, pp. 1–8.

[13] Pfeil A., Böttcher J., Seidl B. E., Heyne J.-P. et al.; *Computer-aided joint space analysis of the metacarpal-phalangeal and proximal-interphalangeal finger joint: normative age-related and gender-specific data*, Skeletal Radiology, 36(9), 2007, pp. 853–864.

[14] Sharp J., Gardner J., Bennett E.; *Computer-based methods for measuring joint space and estimating erosion volume in the finger and wrist joints of patients with rheumatoid arthritis*, Arthritis and Rheumatism, 43(6), 2000, pp. 1378–1386.

[15] Ogiela M. R., Tadeusiewicz R., Ogiela L.; *Image languages in intelligent radiological palm diagnostics*, Pattern Recognition, 39, 2006, pp. 2157–2165.

[16] Tadeusiewicz R., Ogiela M. R.; *Medical image understanding technology*, in: *Studies in fuzzines and soft computing*, Springer, Heidelberg, 2004.

[17] Tadeusiewicz R., Ogiela M. R.; *Picture languages in automatic radiological palm interpretation*, International Journal of Applied Mathematics and Computer Science, 15(2), 2005, pp. 305–312.

[18] Kloster R., Hendriks E. A., Watt I., Kloppenburg M. et al.; *Automatic quantification of osteoarthritis in hand radiographs: validation of a new method to measure joint space width*, Osteoarthritis and Cartilage, 16(1), 2008, pp. 18–25.

[19] Bing Q., Ling-rui T., Jing Z.; *Research on Measurement of Hydrophobocity-of-Insulators*, Proceedings of the CSEE 2008, 26(31), 2008, pp. 120–124.

[20] He C., Lu J., Han J.; *Image edge detection method based on the direction feature of fuzzy entropy*, 2010 Sixth International Conference on Natural Computation, 2010, pp. 3581–3584.

Received December 12, 2010